

# High-energy terahertz pulses from organic crystals: DAST and DSTMS pumped at Ti:sapphire wavelength

B. Monozslai,<sup>1</sup> C. Vicario,<sup>1</sup> M. Jazbinsek,<sup>2</sup> and C. P. Hauri<sup>1,3,\*</sup>

<sup>1</sup>Paul Scherrer Institute, 5232 Villigen PSI, Switzerland

<sup>2</sup>Rainbow Photonics AG, 8048 Zürich, Switzerland

<sup>3</sup>Ecole Polytechnique Federale de Lausanne, 1015 Lausanne, Switzerland

\*Corresponding author: christoph.hauri@psi.ch

Received September 12, 2013; revised October 28, 2013; accepted October 29, 2013;  
posted October 29, 2013 (Doc. ID 197580); published November 25, 2013

High-energy terahertz pulses are produced by optical rectification (OR) in organic crystals 4-dimethylamino-*N*-methyl-4-stilbazolium tosylate (DAST) and 4-*N,N*-dimethylamino-4'-*N'*-methyl-stilbazolium 2,4,6-trimethylbenzenesulfonate (DSTMS) by a Ti:sapphire amplifier system with 0.8  $\mu\text{m}$  central wavelength. The simple scheme provides broadband spectra between 1 and 5 THz, when pumped by a collimated 60 fs near-IR pump pulse, and it is scalable in energy. Fluence-dependent conversion efficiency and damage threshold are reported, as well as optimized OR at visible wavelengths. © 2013 Optical Society of America

OCIS codes: (140.3330) Laser damage; (140.7090) Ultrafast lasers; (190.4400) Nonlinear optics, materials; (190.4410) Nonlinear optics, parametric processes; (190.4710) Optical nonlinearities in organic materials; (320.7110) Ultrafast nonlinear optics.

<http://dx.doi.org/10.1364/OL.38.005106>

One of the recognized concepts for high-field terahertz (THz) generation is based on efficient optical rectification (OR) in organic crystals of mid-IR femtosecond laser pulses [1–3]. While this THz conversion scheme routinely provides THz pulses of megavolt/centimeter field strength, it requires a sophisticated multimillijoule femtosecond mid-IR laser system. The shortage of efficient lasing materials in the wavelength range between 1.3 and 1.5  $\mu\text{m}$  requires the OR pump to be produced by white-light-seeded frequency mixing processes and optical parametric amplifiers, which themselves are pumped by an amplified Ti:sapphire laser [4]. For many applications, however, a less sophisticated laser system is favorable as the pump. In fact, direct pumping of organic crystals by a Ti:sapphire laser would significantly reduce the overall complexity of THz production and provide possibilities for a broader scientific audience. To our best knowledge, OR in organic crystals pumped by a multimillijoule Ti:sapphire system has not yet been considered for high-energy THz pulse generation. State-of-the-art high-energy THz sources are based on LiNbO<sub>3</sub> (up to 125  $\mu\text{J}$ ) [5], but this scheme offers only relatively low THz frequencies (<1 THz). Alternatively, laser-induced gas ionization delivers broadband THz radiation but at limited energy (submicrojoule) [6]. On the other hand, linear accelerator (LINAC)-based sources offer powerful THz radiation at around 0.1–40 THz (up to 100  $\mu\text{J}$ ) [7], but suffer from limited user accessibility.

In this Letter we present results on a simple and compact laser-based multioctave spanning THz generation scheme by OR of an amplified Ti:sapphire pulse in organic 4-dimethylamino-*N*-methyl-4-stilbazolium tosylate (DAST) and 4-*N,N*-dimethylamino-4'-*N'*-methyl-stilbazolium 2,4,6-trimethylbenzenesulfonate (DSTMS) crystals. We perform systematic studies on fluence-dependent conversion efficiencies as well as spectral THz shapes, and give indications on the maximum field and damage threshold of the organic rectifier crystals for a 0.8  $\mu\text{m}$  pump wavelength. We also present THz

measurements close to the optimum visible wavelength for pumping organic crystal.

The experimental setup is illustrated in Fig. 1. For our studies we used a 10 mJ 60 fs Ti:sapphire amplifier system at a 100 Hz repetition rate. The beam is collimated prior to pumping the organic crystals at hand, being a 0.86 mm thick DAST and a 0.2 mm thick DSTMS with 4.5 and 3 mm free apertures, respectively. Unlike other rectification schemes, no pulse front tilting [8] or optical parametric amplifiers are used in our experiment.

The collimated THz radiation is characterized in energy by a calibrated Goly cell, and in the time-frequency domain, by a first-order autocorrelator (AC). The latter offers a broadband bandwidth acceptance in the range of 0.1–20 THz to avoid spectral limitations associated with the crystal-based electro-optic sampling scheme. The instrument is based on a conventional Michelson interferometer, with an additional parabolic mirror before the detector, which is also a Goly cell in our case. Throughout the experiment, a 2 mm thick Teflon filter is used to reduce the background of the pump laser to the detection level of the sensor. All the measurements have been performed at room temperature.

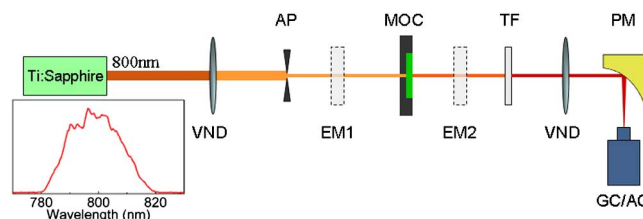


Fig. 1. Schematic of the THz generation setup for organic crystals pumped at 800 nm with a Ti:sapphire amplifier (100 Hz, 10 mJ). VND, Variable neutral density filter wheel; AP, aperture; MOC, mounted organic crystal; TF, Teflon filter; PM, parabolic mirror; EM#, laser energy meter at two positions; and the diagnostics: GC, Goly cell; AC autocorrelator.

The crystal orientation is chosen such that the element  $\chi_{122}^{\text{OR}}$  of the nonlinear susceptibility tensor is employed for OR. While  $\chi_{111}^{\text{OR}}$  offers the most efficient THz generation when pumped with short wavelength IR (SWIR) radiation between 1.3 and 1.5  $\mu\text{m}$  (490  $\text{pm}/\text{V}$ ), the index  $\chi_{122}^{\text{OR}}$  is best suited for near-IR pumping (700–800 nm), as predicted in [9] and experimentally confirmed in [10].

The highest conversion efficiency is provided for perfect velocity matching between the THz phase velocity and the group velocity of the optical pump pulse, which is equivalent to being parallel to the crystal  $b$  axis. For  $\chi_{122}^{\text{OR}}$  at 800 nm, a value of 166  $\text{pm}/\text{V}$  is reported [11,12]. This indicates less efficient OR than with a SWIR pump.

Figure 2 shows the THz pulse energy and the near-IR-to-THz conversion efficiency as functions of the pump fluence for DAST and DSTMS. The measured THz energy increases almost linearly with respect to the pump fluence to 100 nJ for DAST (15.9  $\text{mm}^2$  emitter surface) and 50 nJ for DSTMS (7.1  $\text{mm}^2$  emitter surface) at 17 and 14  $\text{mJ}/\text{cm}^2$  pump fluencies, respectively. Please note that these values were measured after 2 mm Teflon filter, and are not corrected with the  $\sim 25\%$  average absorption across the 0.3–5 THz range. Up to this fluence, which is close to the damage threshold, no saturation could be observed in the THz energy. The conversion efficiency, shown in Fig. 2(b), increases slightly for higher pump fluence and levels of  $6\text{e-}5$  for DSTMS and  $4\text{e-}5$  for DAST, respectively. Shown in Fig. 3 are typical THz spectra recorded for OR with the 800 nm pump. The output covers 1–5 THz and peaks around 2 THz.

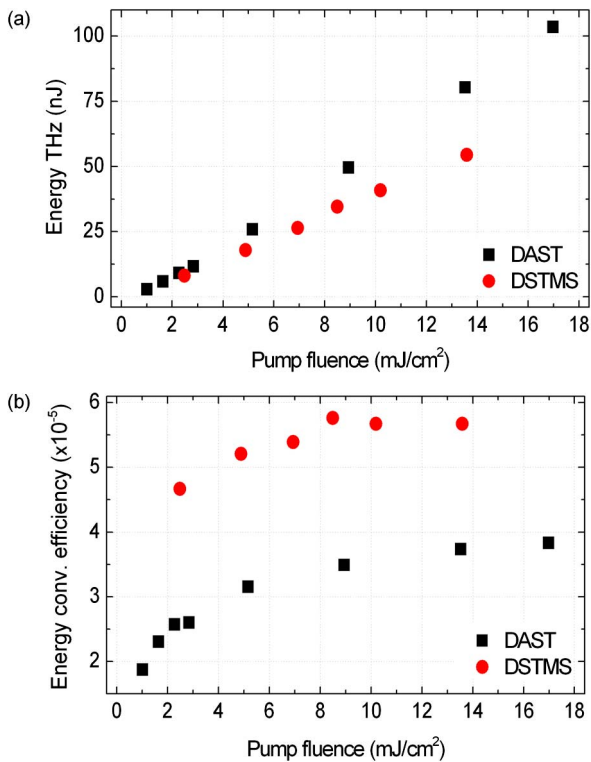


Fig. 2. Background-corrected (a) THz pulse energy and (b) corresponding conversion efficiencies as functions of the applied Ti:sapphire pump fluence for DAST and DSTMS, with emitting surfaces of 15.9 and 7.1  $\text{mm}^2$ , respectively. Measured after a 2 mm Teflon plate.

In the experiment, only a weak spectral content is observed at frequencies lower than the phonon-active mode at 1.1 THz. The overall spectral response is in acceptable agreement with the theoretically expected spectral output (dashed lines), which considers the crystal thickness, pulse duration, and pump wavelength. Shown in Fig. 3 is an overview on the theoretically expected spectral content produced in DAST and DSTMS as functions of the pump laser wavelength. The calculated curves are based on velocity matching and linear THz absorption in the crystal [9,12]. We associate the small discrepancy between experimental and theoretical results, observed in particular for DAST [see Fig. 3(a)], to the fact that effects like nonlinear absorption and cascading are not treated in the numerical calculation.

The highest pump fluence used in the experiment is close to the measured damage threshold. For 68 fs pulses (FWHM) at 800 nm, a damage threshold of 300  $\text{GW}/\text{cm}^2$  (20  $\text{mJ}/\text{cm}^2$ ) was measured for DAST, and slightly lower value was found for DSTMS.

Although the electric field shape was not measured, the maximum field strength can be estimated by the pulse energy and its spectral content. With a strongly focused spot size, an electric field of 1  $\text{MV}/\text{cm}$  [13] is calculated. This field strength has been shown sufficiently high to initiate nonlinear THz phenomena [14–18]. Previous works have shown that the focusability of THz radiation from organic crystal emitters is excellent, mainly due to the simple generation scheme. The resulting THz beam properties, such as a nondistorted pulse wave front and identical divergence for both lateral dimensions, help to achieve diffraction limited spot sizes. In principle, higher THz pulse energies become feasible

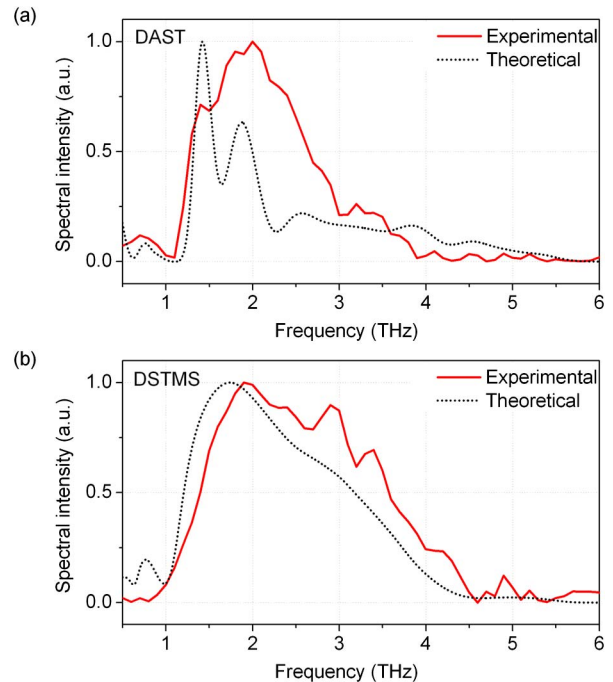


Fig. 3. THz spectra for (a) DAST and (b) DSTMS pumped at 800 nm (fluence 6  $\text{mJ}/\text{cm}^2$ ) along the  $b$  axis. The theoretical results were corrected for the transmission of the 2 mm thick Teflon sheet.

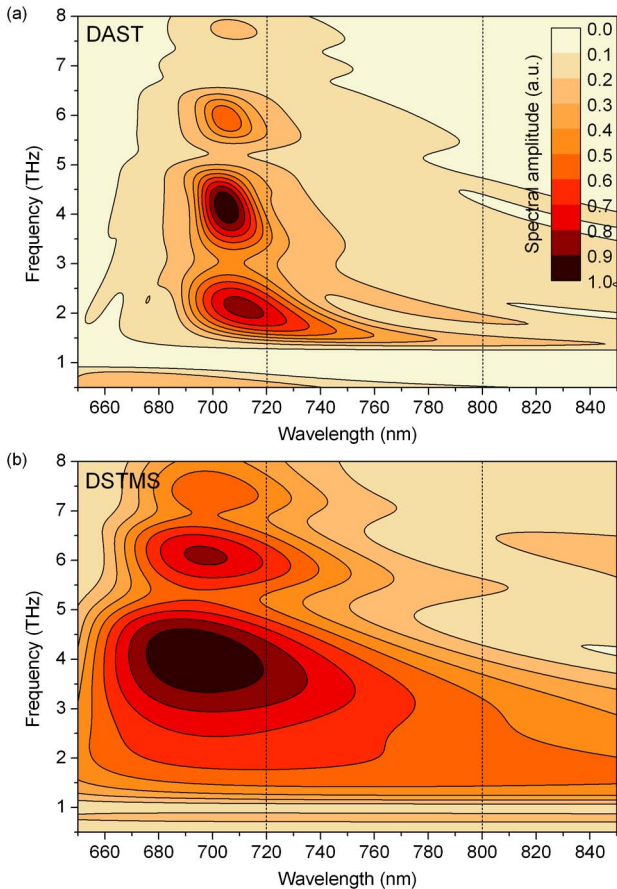


Fig. 4. Calculated spectral amplitudes of the THz frequency components (normalized) as a function of the pump wavelength, in the case of (a) 0.86 mm thick DAST and (b) 0.2 mm thick DSTMS. The vertical dashed lines show the pump laser wavelengths used in the presented investigation.

when scaling the size of the crystal. For a crystal with a 10 mm clear aperture, a THz pulse energy of 0.5  $\mu\text{J}$  is expected, corresponding to a field of 2.3 MV/cm. The growing of such large crystal sizes has recently become feasible. This scheme could be a potential alternative to large-scale LINAC-based THz sources, in terms of electric field.

Finally we present studies on the visible wavelengths that are best suited to achieve broadband and efficient THz radiation. In fact, as indicated by Fig. 4, the most effective visible pump laser wavelengths for broadband OR in organic crystals are located around 680–740 nm for DAST and around 700 nm for DSTMS. Unfortunately, these wavelengths are outside the typical gain bandwidth of a commercially available Ti:sapphire amplifier.

However, in order to verify the theoretical expectations, THz spectra were recorded for a pump wavelength of 720 nm for DAST and DSTMS, using the frequency-doubled signal from an optical parametric amplifier. As predicted by Fig. 4, under these conditions velocity matching is fulfilled also for higher THz frequencies, resulting in multioctave spanning spectra covering 0.5–5 THz. The corresponding experimental results are shown in Fig. 5. At this visible pump wavelength the expected conversion efficiency is 10 (2.5) times higher for DAST (DSTMS) compared to pumping at 800 nm.

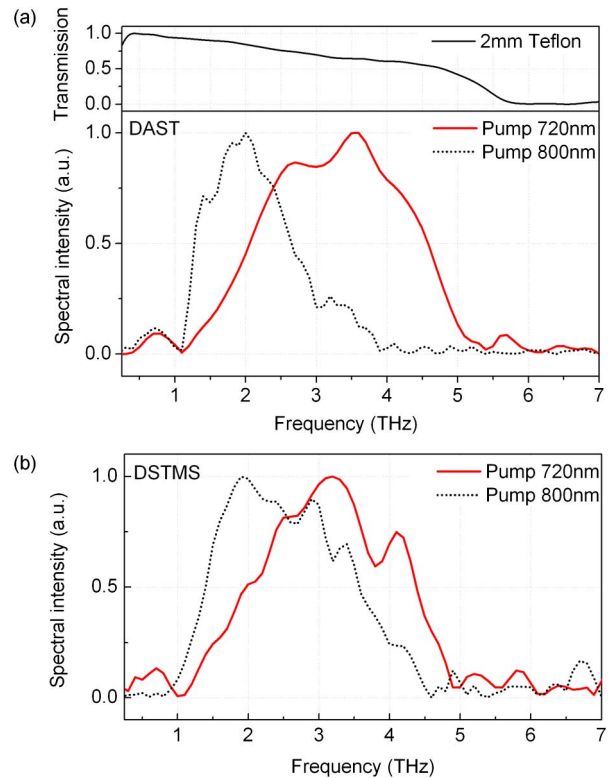


Fig. 5. Measured THz spectra for (a) DAST and (b) DSTMS pumped at 720 and 800 nm. For visible pumping, the spectrum is limited by the Teflon transmission, cutting off for frequencies  $>5$  THz, as shown in (a).

Finally, we would like to mention that the crystal thickness also has a strong influence on the rectified spectral components due to the phase-matching conditions. Figure 6 gives an overview of the maximum effective lengths for THz wave generation as defined in [9], as a function of the pump wavelength. With crystals thinner than those available for our investigation, phase matching over a broader spectral range could be achieved.

In conclusion, we have investigated the generation of high-energy THz pulses in organic crystals (DAST and DSTMS) pumped by a conventional Ti:sapphire laser. Broadband THz radiation of up to 5 THz has been demonstrated with pulse energies of up to 0.1  $\mu\text{J}$  (on target), and damage thresholds were reported. Furthermore, we demonstrated the possibility of generating higher THz

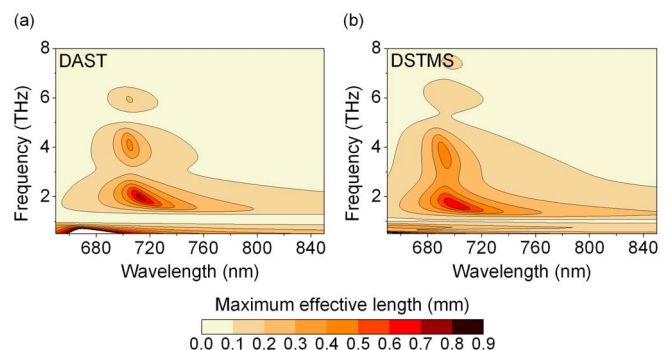


Fig. 6. Maximum effective length for efficient THz generation in (a) DAST and (b) DSTMS along the  $b$  axis, for visible/near-IR pumping wavelengths.

frequencies by using a pump laser wavelength of 720 nm. The measured efficiencies are comparable to other ordinary OR crystals, like the semiconductor ZnTe ( $3.1e - 5$ ) [19]. Even higher efficiencies could be expected for optimized crystal thickness. Although LiNbO<sub>3</sub>-based sources show slightly better conversion efficiencies [8], the organic crystals allow accessing significantly higher frequencies, well beyond 1 THz, and they work without pulse front tilting. Due to its simplicity, the presented source is of interest for both spectroscopic and high-field applications. It furthermore opens new opportunities in scaling THz sources toward higher field strength, thanks to the increasing availability of commercial Ti:sapphire systems at the terawatt power level.

We are grateful to C. Medrano and B. Ruiz from Rainbow Photonics for fruitful discussions. This work was supported by the SNSF (grant no. 51NF40-144615) in the framework of NCCR-MUST and by the SwissFEL. B. M. acknowledges support from the Sciex-NMS (grant no. 12.159). C. P. H. acknowledges support from the Swiss National Science Foundation (grant no. PP00P2\_128493).

#### References and Notes

1. C. P. Hauri, C. Ruchert, C. Vicario, and F. Ardana, *Appl. Phys. Lett.* **99**, 161116 (2011).
2. C. Ruchert, C. Vicario, and C. P. Hauri, *Phys. Rev. Lett.* **110**, 123902 (2013).
3. C. Vicario, C. Ruchert, and C. P. Hauri, *J. Mod. Opt.* **60**, 1 (2013).
4. A. Trisorio, P. M. Paul, F. Ple, C. Ruchert, C. Vicario, and C. P. Hauri, *Opt. Express* **19**, 20128 (2011).
5. J. A. Fülöp, L. Pálfalvi, S. Klingebiel, G. Almási, F. Krausz, S. Karsch, and J. Hebling, *Opt. Lett.* **37**, 557 (2012).
6. M. Clerici, M. Peccianti, B. E. Schmidt, L. Caspani, M. Shalaby, M. Giguère, A. Lotti, A. Couairon, F. Légaré, T. Ozaki, D. Faccio, and R. Morandotti, *Phys. Rev. Lett.* **110**, 253901 (2013).
7. D. Daranciang, J. Goodfellow, M. Fuchs, H. Wen, S. Ghimire, D. A. Reis, H. Loos, A. S. Fisher, and A. M. Lindenberg, *Appl. Phys. Lett.* **99**, 141117 (2011).
8. M. Kunitski, M. Richter, M. D. Thomson, A. Vredenburg, J. Wu, T. Jahnke, M. Schöffler, H. Schmidt-Böcking, H. G. Roskos, and R. Dörner, *Opt. Express* **21**, 6826 (2013).
9. A. Schneider, M. Neis, M. Stillhart, B. Ruiz, R. U. A. Khan, and P. Günter, *J. Opt. Soc. Am. B* **23**, 1822 (2006).
10. X. M. Zheng, C. V. McLaughlin, P. Cunningham, and L. M. Hayden, *J. Nanoelectron. Optoelectron.* **2**, 58 (2007).
11. F. Pan, G. Knopfle, Ch. Bosshard, S. Follonier, R. Spreiter, M. S. Wong, and P. Gunter, *Appl. Phys. Lett.* **69**, 13 (1996).
12. A. Schneider, "Generation and detection of terahertz pulses in organic crystals," dissertation no. 16132 (ETH, 2005).
13. We assumed  $f = 50$  mm focusing optics with a numerical aperture of 1, 0.5 ps pulse duration, 2 THz central frequency, and 0.1  $\mu$ J THz pulse energy.
14. C. Vicario, C. Ruchert, F. Ardana-Lamas, P. M. Derlet, B. Tudu, J. Luning, and C. P. Hauri, *Nat. Photonics* **7**, 720 (2013).
15. A. Dienst, M. C. Hoffmann, D. Fausti, J. C. Petersen, S. Pyon, T. Takayama, H. Takagi, and A. Cavalleri, *Nat. Photonics* **5**, 485 (2011).
16. T. Kampfrath, A. Sell, G. Klatt, A. Pashkin, S. Mährlein, T. Dekorsy, M. Wolf, M. Fiebig, A. Leitenstorfer, and R. Huber, *Nat. Photonics* **5**, 31 (2011).
17. B. D. Patterson, J. Sa, A. Ichsanow, C. P. Hauri, C. Vicario, C. Ruchert, C. Izabela, R. Gehrig, H. C. Sigg, J. van Bokhoven, and R. Abela, *Chimia* **65**, 323 (2011).
18. D. Turchinovich, J. M. Hvam, and M. C. Hoffmann, *Proc. SPIE* **8260**, 82600G (2012).
19. F. Blanchard, L. Razzari, H. C. Bandulet, G. Sharma, R. Morandotti, J. C. Kieffer, T. Ozaki, M. Reid, H. F. Tiedje, H. K. Haugen, and F. A. Hegmann, *Opt. Express* **15**, 13212 (2007).